Int. J. Miner. Process. 88 (2008) 1–6

Contents lists available at ScienceDirect

Int. J. Miner. Process.

journal homepage: www.elsevier.com/locate/ijminpro

Structural changes in olivine (Mg, Fe)$_2$SiO$_4$ mechanically activated in high-energy mills

Peter Baláž [a,*], Erika Turianicová [a], Martin Fabián [a], Rolf Arne Kleiv [b], Jaroslav Briančin [a], Abdullah Obut [c]

[a] Institute of Geotechnics, Slovak Academy of Sciences, Watsonova 45, 043 53 Košice, Slovakia
[b] Norwegian University of Science and Technology, Sem Sælandsvei 1, N-7491 Trondheim, Norway
[c] Hacettepe University, Mining Engineering Department, 06800 Beytepe, Ankara, Turkey

ARTICLE INFO

Article history:
Received 14 June 2007
Received in revised form 25 February 2008
Accepted 7 April 2008
Available online 12 April 2008

Keywords:
Olivine
Mechanical activation
Milling
Carbon dioxide
Sequestration
Structure

ABSTRACT

This study evaluates the structural changes in olivine (Mg, Fe)$_2$SiO$_4$ (deposit Åheim, Norway) generated by its mechanical activation. The high-energy milling in laboratory planetary and attrition mills as well as in an industrially nutating mill was applied during activation. To identify mechanically-induced changes in the mineral, scanning electron microscopy (SEM), X-ray diffraction (XRD), specific surface area measurement and infrared spectroscopy (IR) techniques have been used. The observed physico-chemical changes illustrate the possibility to modify the surface and/or volume properties of olivine depending on the applied activation mode. Infrared spectroscopy seemed to be suitable method for characterization of CO_2 absorption modified on olivine.

1. Introduction

The increasing atmospheric CO_2 concentration, mainly caused by fossil fuel combustion, has led to concerns about global warming (Huijgen et al., 2005). During the last 60 years, CO_2 concentrations increased over 30% compared to pre-industrial levels. Consequently, the focus has been placed on managing CO_2 emissions. Carbon management can be achieved through three different, but complimentary approaches: increasing the efficiency of energy conversion, using low-carbon or carbon-free energy sources and sequestering CO_2 emissions. There is strong tendency to develop technologies with a possibility to achieve zero emissions (Maroto-Valer et al., 2005). The idea of CO_2 sequestration was originally proposed by Seifritz (Seifritz, 1990) and first studied in more details by Lackner (Lackner et al., 1995). The basic concept behind CO_2 mineral sequestration is to mimic natural weathering processes in which Ca- or Mg-containing minerals are converted into Ca- or Mg-carbonates (Huijgen et al., 2005) as exemplified by the following equation

$$(Ca, Mg)SiO_3 + CO_2 \rightarrow (Ca, Mg)CO_3 + SiO_2. \quad (1)$$

The formed mineral carbonates are known to be stable over geological time periods (of thousands to millions of years).

There are several calcium and/or magnesium silicates suitable as mineral feedstock, e.g. wollastonite $CaSiO_3$, enstatite $MgSiO_3$, forsterite Mg_2SiO_4, fayalite Fe_2SiO_4, olivine (Mg, Fe)$_2$SiO$_4$, diopside $CaMgSi_2O_6$, talc $Mg_3SiO_{10}(OH)_2$ and serpentine $Mg_3Si_2O_5(OH)_4$.

However, under ambient conditions the process of silicate minerals conversion according to Eq. (1) is slow and a significantly higher extent of sequestration reactions and faster conversion rates are needed for its technical feasibility (Huijgen et al., 2006).

Enhancement of the chemical process by mechanical activation can results in major improvement of the reaction rate (Baláž, 2000). The potential of mechanical activation lies in its possibility to control and regulate the course of heterogeneous processes by the complex influence on solids via formation of different defects like a new surface area, dislocations, point defects, etc. There are several studies aimed at improving the pretreatment of various silicates by mechanical activation performed by high energy milling in order to improve their CO_2 sequestration (O'Connor et al., 1999, 2000, 2002, 2004; Kalinkina et al., 2001; Kalinkin et al., 2003, 2004; Hredzák et al., 2004, 2005; Park and Fan, 2004; Kleiv and Thornhill, 2006; Kleiv et al., 2006; Zhang et al., 1997).

The aim of the present paper is to investigate the physico-chemical properties of olivine mechanically activated in laboratory and industrial mills. The various experimental techniques will be applied to identify mechanically-induced changes in olivine structure.

* Corresponding author. Tel.: +421 55 7922603; fax: +421 55 7922604.
E-mail address: balaz@saske.sk (P. Baláž).

0301-7516/$ – see front matter © 2008 Elsevier B.V. All rights reserved.
doi:10.1016/j.minpro.2008.04.001

2. Experimental

2.1. Material

The olivine sample used in this study was kindly supplied by the North Cape Minerals company and originated from the production plant at Åheim (Norway). The sample of 95% purity contains approximately 93% forsterite Mg_2SiO_4 and 7% fayalite Fe_2SiO_4. Small amounts of accessory minerals like chlorite, chromite, enstatite, serpentinite and talc can also be found in the sample.The bulk chemical composition of the sample under study is shown in Table 1.

2.2. Mechanical activation

The olivine sample was mechanically activated in three high energy mills:

- *Laboratory planetary mill Pulverisette 6 (Fritsch, Germany)* with loading of the mill with 50 balls of 10 mm diameter; material of 250 ml milling chamber and balls: WC. Weight of milling balls and sample was 360 and 18 g, respectively. The mill was run at the planet carrier rotation speed 450 revs min^{-1} for milling times of 2–30 min and was operated at ambient temperature and free access of air.
- *Laboratory attritor mill Molinex PE 075 (Netzsch, Germany)* with 500 ml milling chamber which contained 100 g of sample and 2000 g of 2 mm diameter stainless balls and 100 ml of water. The mill was running at rotation speed 1500 revs min^{-1} for milling times of 5–120 min and was operated at ambient temperature and free access of air.
- *Industrial nutating mill Hicom 15 (Hicom International Pty, Ltd., Australia)* with 5000 ml milling chamber and milling charge of 1 kg of sample. The mill was run at 900 revs min^{-1} using mixture of 10 kg of 5 mm and 2 kg of 20 mm diameter stainless steel balls. The mill was operated in a dry mode and at ambient temperature and free access of air. In several experiments the milling was performed with the presence of H_2O (50, 100, 200 and 500 ml, respectively).

2.3. Specific surface area

The specific surface area was determined by the low temperature nitrogen adsorption method in a Gemini 2360 sorption apparatus (Micromeritics, USA).

2.4. Scanning electron spectroscopy

The scanning electron microscopy (SEM) was carried out with a BS 340 (Tesla Brno, Czech Republic).

2.5. X-ray diffractometry

The X-ray diffraction measurements were carried out using a diffractometer X´Pert (Philips, Netherlands) working in the 2Θ geometry with CuKα radiation. The XRD lines were identified by comparing the measured patterns to the JCPDS data cards. The effect of mechanical activation was evaluated by the decrease of crystalline phase X of the olivine

$$X = \frac{U_0}{I_0} \cdot \frac{I_x}{U_x} \cdot 100(\%) \quad (2)$$

where U_0 and U_x denote the background of the reference and activated sample, while I_0 and I_x are integral intensities of selected diffraction lines of reference sample and activated sample, respectively (Ohlherg and Strickler, 1962).

2.6. Infrared spectroscopy

The IR spectroscopy measurements were carried out using a FT-IR Avatar 330 spectrometer (Thermo-Nicolet, USA) using KBr technique for preparation samples.

3. Results and discussion

3.1. Changes in surface area

Mechanical activation of olivine was performed in planetary (PM), attritor (AM) and nutating (NM) mills and the dependence of specific surface area S_A of the samples on the time of mechanical activation is represented in Figs. 1–3. These plots show that the new surface formation is affected by both the time of mechanical activation and the milling conditions (type of mill). We can see the increase in specific surface area for the olivine sample milled in an attrition mill (Fig. 1) is much higher than for the sample

Table 1
The chemical composition of the olivine sample

Component	%
MgO	50.2
SiO_2	41.5
Fe_2O_3	7.41
Cr_2O_3	0.30
Al_2O_3	0.36
NiO	0.33
MnO	0.08
CaO	0.08
Na_2O	0.01
K_2O	0.01

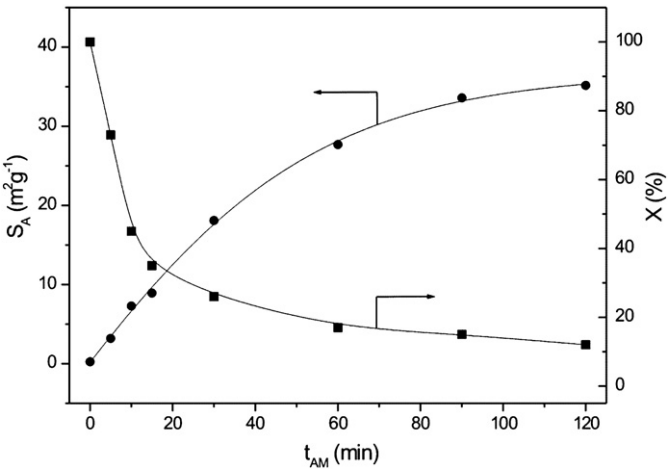

Fig. 1. Specific surface area S_A and content of crystalline phase X of olivine as a function of milling time t_{AM} in an attritor.

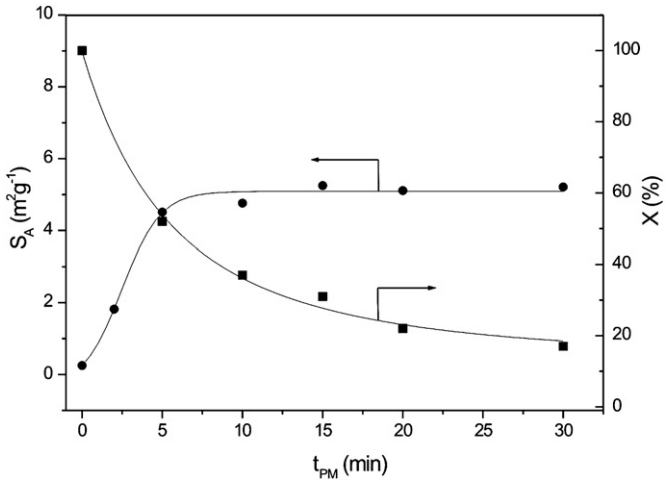

Fig. 2. Specific surface area S_A and content of crystalline phase X of olivine as a function of milling time t_{PM} in a planetary mill.

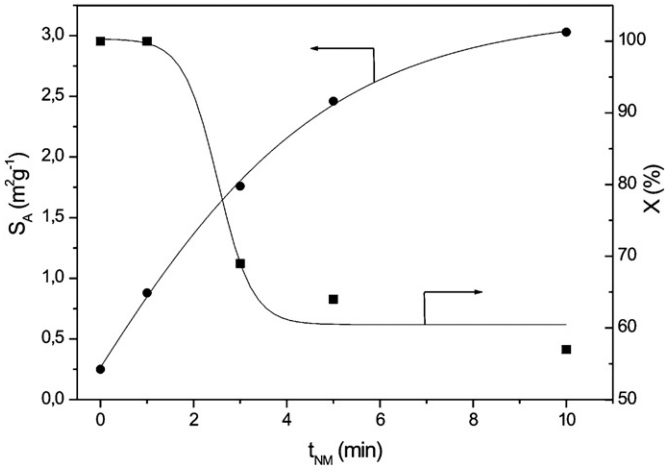

Fig. 3. Specific surface area S_A and content of crystalline phase X of olivine as a function of milling time t_{NM} in a nutating mill.

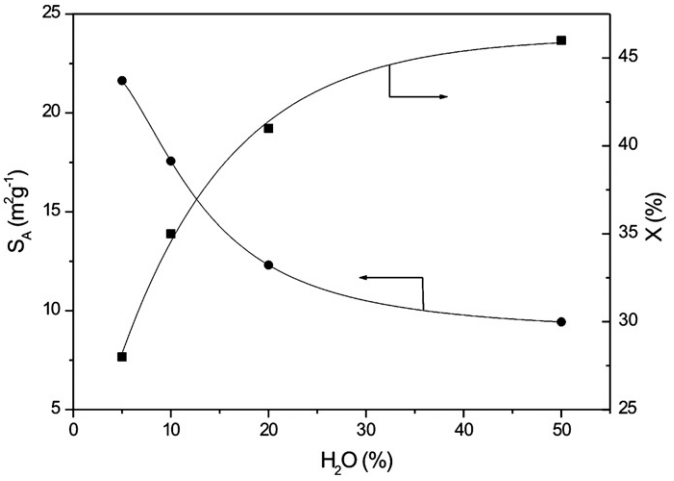

Fig. 4. Specific surface area S_A and content of crystalline phase X of olivine as a function of H_2O addition by nutating milling.

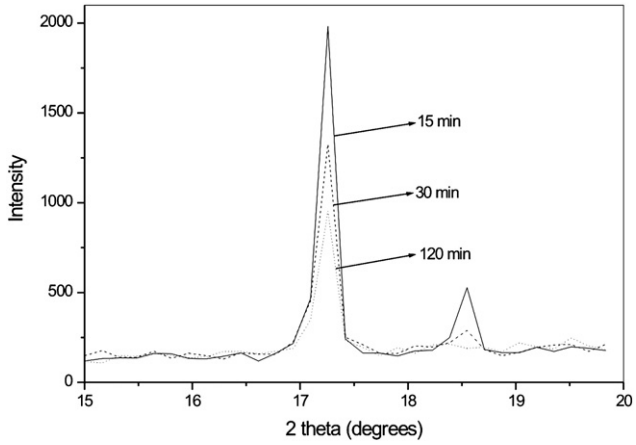

Fig. 6. XRD pattern of olivine (020) peak as a function of milling time in an attritor.

milled in planetary and nutating mills (Figs. 2–3). The disintegration of olivine by mechanical activation is accompanied by an increase in the number of particles and by the generation of fresh, previously unexposed surface (Park and Fan, 2004; Kleiv and Thornhill, 2006). By application of the three mills the common features in plots in Figs. 1–3 can be identified. After the first stage where the increase in surface area is almost proportional to the milling time, the second stage is manifested. Here, the new surface area formation is slow down. This effect is the most pronounced in a planetary mill and in literature is attributed to particle enlargement (aggregation and/or agglomeration). In some cases when the very intensive milling is applied, the changes in the crystal structure and mechanochemical reactions appear in this stage (Baláž, 2000; Beke, 1984; Juhász and Opoczky, 1990; Tkáčová, 1989).

Special effect has been observed by milling of olivine for 10 min in nutating mill in the presence of small amounts of water (Fig. 4). The less water is applied, the higher values for specific surface area (S_A) have been obtained: for 5%(w/w) H_2O the value of S_A was 21.6 m^2g^{-1} which is comparable with values obtained by wet milling in an attritor (Fig. 1). The effect of the addition of small amounts of a liquid to accelerate the solid-state reactions carried out by milling is called kneading in the chemical engineering. Kneading has been described as a sort of catalysis, where the small amount of solvent provides a lubricant for solid-state diffusion (Braga and Grepioni, 2004, 2005).

Fig. 5 illustrates scanning electron micrographs (SEM) of the as-received (a) as well as mechanically activated (b–d) olivine samples. The as-received sample shows particles irregular in shape with characteristic sharp edges. During milling the particles are rounded, fractured and diminished. Some large particles still exist but an overall reduction in size appears to have occurred as a result of high-energy milling. The attritor milled samples (b) show the most significant reduction in size which is in agreement with the results of olivine milling published in paper (Summers et al., 2005). In some cases (c, d) the evidence of well-bonded aggregates can be seen.

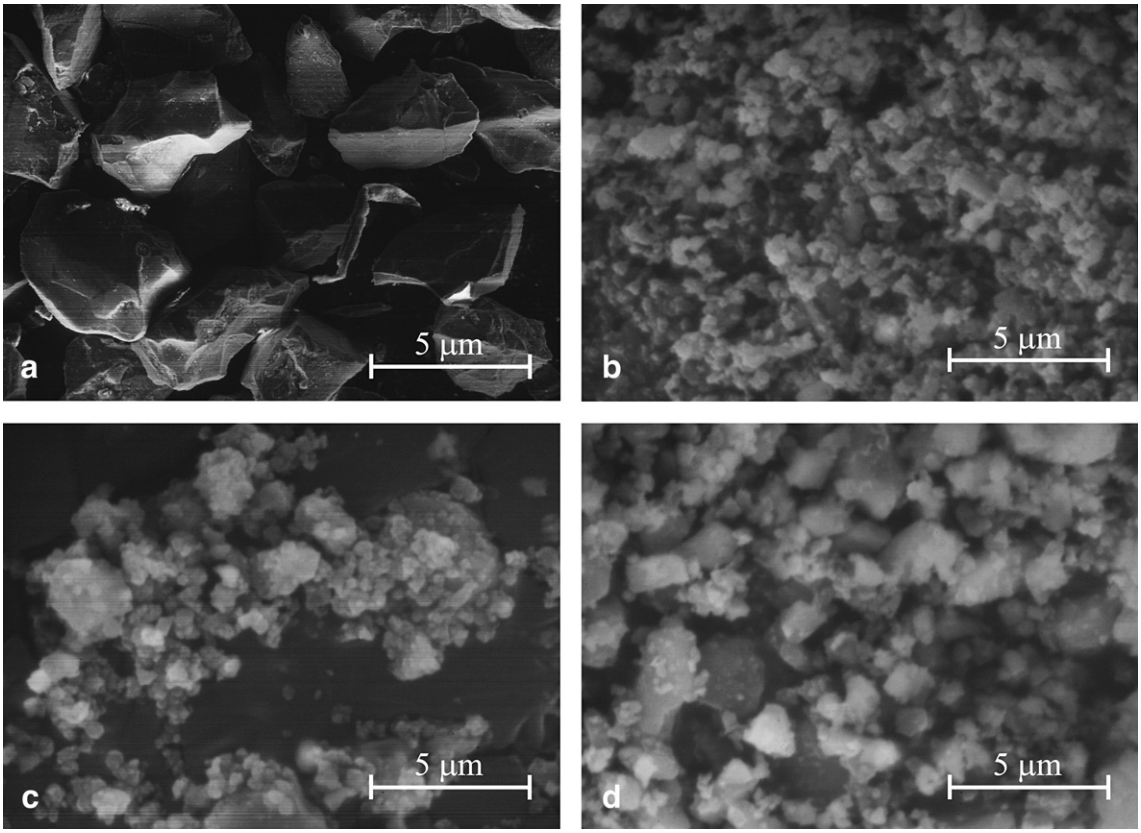

Fig. 5. SEM photographs of olivine: (a) as-received sample, (b–d) samples after milling in attritor mill, planetary mill and nutating mill, respectively.

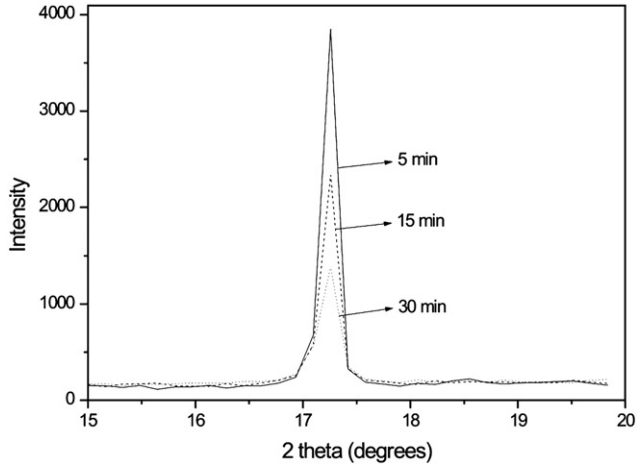

Fig. 7. XRD pattern of olivine (020) peak as a function of milling time in a planetary mill.

3.2. Changes in crystal structure

To appreciate the lattice defect deformation in the bulk of olivine several physico-chemical methods can be used. The application of the XRD method enables us to investigate the disordering of olivine crystal structure during high-energy milling. The induced changes can be observed by looking at the line broadening, the reduction of peaks intensity and the shift of XRD peaks (Baláž, 2000; Tkáčová, 1989; Pourghahramani and Forssberg, 2006a,b).

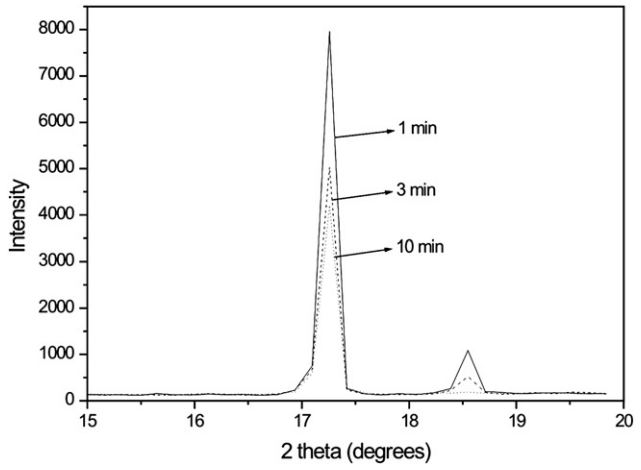

Fig. 8. XRD pattern of olivine (020) peak as a function of milling time in a nutating mill.

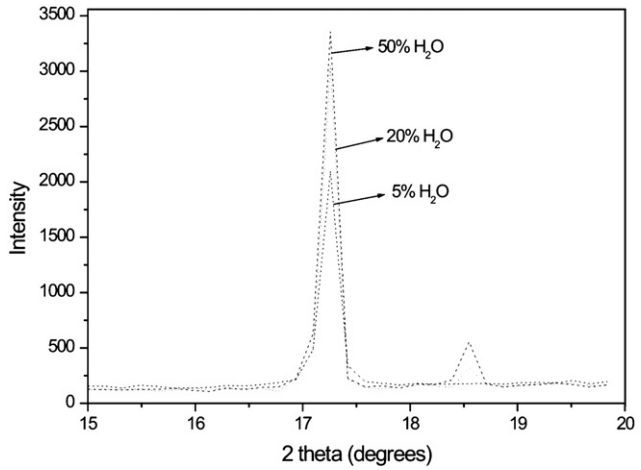

Fig. 9. XRD pattern of olivine (020) peak as a function of H_2O addition by nutation milling.

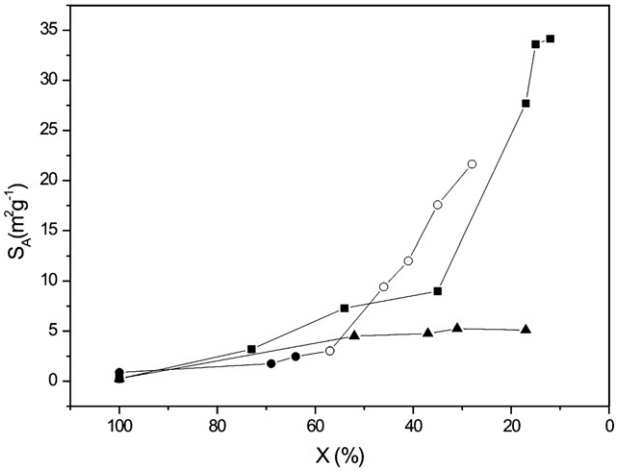

Fig. 10. Specific surface area S_A of olivine as a function of content of crystalline phase X. (■) attritor mill, (▲) planetary mill, (●) nutating mill (dry milling), (○) nutating mill (wet milling with H_2O).

The results obtained from XRD measurements show a large reduction in selected olivine peak height together with line broadening with increasing activation time (Figs. 6–9). Decrease of the crystalline phase content X as a measure of olivine disordering has been calculated according to the Eq. (2). The dependence of the calculated values of X on the time of mechanical activation is shown in Figs. 1–3. In Fig. 4 the dependence of X as a function of H_2O addition by nutating milling is shown. In all cases of high-energy milling, disordering in the bulk of olivine increases with the time of mechanical activation (the values of X are diminishing).

The decrease in crystalline phase X values 100% to 12%, 100% to 17% and 100% to 57% for attrition, planetary and nutating milling (dry mode) have been documented. The differences between the mills result from changes in milling conditions. Generally, the observed trend manifested by plots in Figs. 1–3 is well documented in mechanochemical monographs (Baláž, 2000; Tkáčová 1989).

The mutual dependence of new surface area S_A formation and the content of crystalline phase X of the mechanically activated olivine in various mills is depicted in Fig. 10. From this Figure is evident, that the products of milling in the attritor, planetary

Table 2
The milling parameters and physico-chemical properties of the olivine sample

Type of mill	Revolutions (revs min^{-1})	Milling time (min)	H_2O addition (ml)	Specific surface area S_A (m^2g^{-1})	Crystalline phase, X (%)	Milling energy, E (kW h kg^{-1})
As received sample	–	–	–	0.25	100	–
Attritor	1500	5	100	3.2	73	0.09
	1500	10	100	7.3	45	0.19
	1500	15	100	8.9	35	0.29
	1500	30	100	18.1	26	0.58
	1500	60	100	27.7	7	1.15
	1500	90	100	33.6	15	1.73
	1500	120	100	35.2	12	2.31
Planetary mill	450	2	–	1.8	85	0.40
	450	5	–	4.5	52	1.00
	450	10	–	4.8	37	2.01
	450	15	–	5.3	31	3.02
	450	20	–	5.1	22	4.02
	450	30	–	5.2	17	6.03
Nutating mill	900	1	–	0.9	100	0.06
	900	3	–	1.8	69	0.19
	900	5	–	2.5	64	0.32
	900	10	–	3.0	57	0.64
	900	10	50	21.6	100	0.72
	900	10	100	17.6	86	0.71
	900	10	200	12.3	41	0.65
	900	10	500	9.4	46	0.51

Values of milling energy have been calculated according to the equations given for attritor and planetary mill in paper (Pourghahramani and Forssberg, 2006a). Values for the nutating mill have been calculated from the values of power input measured continuously during the milling experiments.

mill and nutating mill differ in a specific structural deterioration. Milling in wet mode (attritor and several experiments in the nutating mill) show the highest values of specific surface area. The two-stage process of the new surface area formation can be deduced from the plots in Fig. 10. In the first stage characteristic for dry milling, the increase of S_A values with olivine deterioration (decrease of X values) is very small. In the second stage characteristic for wet milling (in presence of H_2O) only small changes in values of X bring about the massive increase of S_A. However, some limiting values of X are required in this case: X<55% and X<35% for nutating mill and attritor mill, respectively.

Summary of the milling results is given in Table 2. Milling in an attritor seemed to be very promising from the point of view of induced physico-chemical changes: both S_A and X values are the most different in comparison with as received sample (S_A=35.2 m^2g^{-1} vs. 0.25 m^2g^{-1} and X=12% vs. 100%). The same is valid for the maximum value of crystalline phase at planetary milling (X=17%). The corresponding values of milling energy for attritor and planetary mill are relatively high in comparison with the values for nutatting milling. However, the values of S_A and X are not the same. The future studies on mill selection in connection with effective CO_2 sequestration are needed.

3.3. Infrared spectroscopy

Fig. 11 shows the infrared spectra of non-activated (1) and mechanically activated (2–4) olivine. Three regions of IR-bands can be identified. In the first region there is an intensive band with maximum at 3500 cm^{-1} which corresponds to OH− vibrations as a result of hydration of olivine. No differences in intensity of this band have been detected for samples without or with application of the drying step during preparation of samples for IR measurements. Therefore the water molecules seemed to be bound by chemisorption. The intensity of this band rises with increasing of olivine disordering by milling. The most intensive band is for sample 4 with the highest value of specific surface area S_A and the lowest value of X (see inset in Fig. 11). The second region with 1100–500 cm^{-1} is characteristic for olivine (Gadsden, 1975; Nakamoto, 1978; Boldyrev, 1976). There is the same tendency in shape of spectra as described for the first region. There are 3 bands in the third region (Fig. 12). However, none of them is intrinsic to the non-activated olivine and their appearance is connected with the mechanical activation. The band at 1630 cm^{-1} belongs to H_2O vibration mode. We speculate that a double peak in range 1510–1430 cm^{-1} could hidden a characteristic double peak in the 1515–1430 cm^{-1} region attributable to carbonate absorption (Kalinkin et al., 2003, 2004; Fine and Stolper, 1986; Shi et al., 2005) as a consequence of CO_2 presence in air during milling. If this absorption is direct or proceeds through an interaction with chemisorbed water is not clear and needs further investigation.

4. Conclusions

- Changes in the surface area and morphology of olivine samples were detected as a consequence of high-energy milling. Milling in the wet mode show the higher values of specific surface area.
- The application of XRD method enabled monitoring of the bulk changes induced in olivine samples during milling. The results obtained show a large reduction in selected (020) olivine peak intensity with increasing milling time which manifest decrease in content of crystalline phase of the mineral.

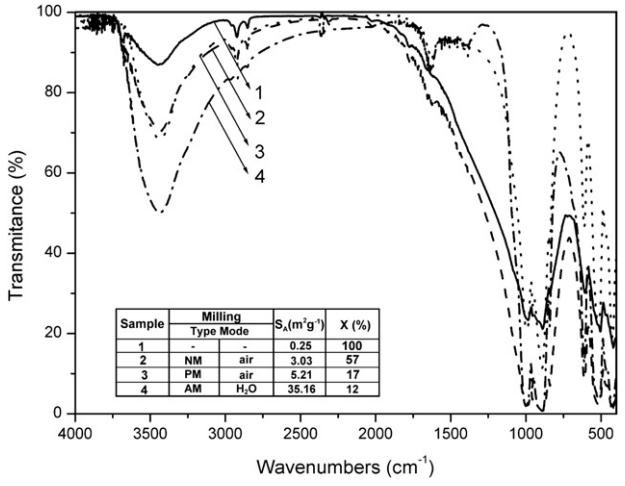

Fig. 11. FT-IR spectra of olivine: (1) initial, (2, 3, 4) after milling in planetary mill, nutating mill and attritor, respectively.

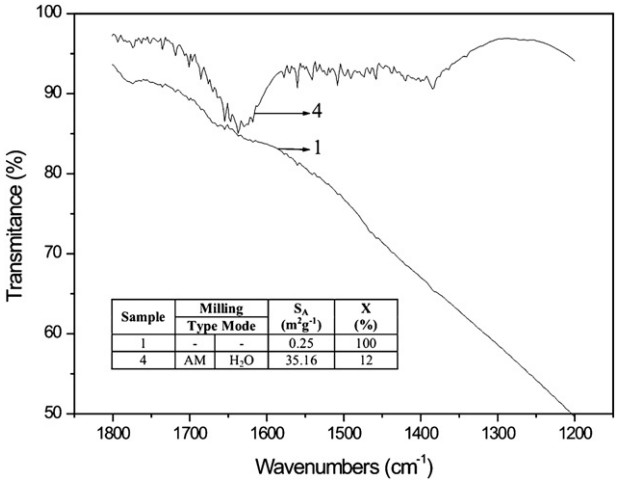

Fig. 12. FT-IR spectra of olivine: (1) initial, (4) after attritor milling. Characteristic bands for CO_2 are shown.

- The infrared spectroscopy offers a possibility to monitor carbonate absorption which is a suitable identification tool for future CO_2 sequestration studies.

Acknowledgments

The support through the Slovak Research and Developing Agency APVV (project LPP - 0196 - 06), the Slovak Grant Agency VEGA (project 2/0035/08) and Center of Excellence of the Slovak Academy of Sciences (NANOSMART) is gratefully acknowledged as is the support through the Norwegian ENGAS Research Infrastructure (NTNU-SINTEF). This manuscript benefited from the comments of three reviewers.

References

Baláž, P., 2000. Extractive Metallurgy of Activated Minerals. Elsevier, Amsterdam.
Beke, B., 1984. Consideration about the energetic effectivity of fine grinding. Proc. International Symposium on Powder Technology, Kyoto 1981. Hemisphere Publishing Corporation, Washington, pp. 373–379.
Boldyrev, A.I., 1976. Infrared Spectra of Minerals. Nedra, Moscow. (in Russian).
Braga, D., Grepioni, F., 2004. Reactions between or within molecular crystals. Angewandte Chemie International Edition 43, 4002–4011.
Braga, D., Grepioni, F., 2005. Making crystals from crystals: a green route to crystal engineering and polymorphism. Chemical Communications 3635–3645.
Fine, G., Stolper, E., 1986. Dissolved carbon dioxide in basaltic glasses: concentrations and speciation. Earth and Planetary Science Letters 76, 263–278.
Gadsden, J.A., 1975. Infrared Spectra of Minerals and Related Inorganic Compounds. Butterworth, London.
Hredzák, S., Jakabský, Š., Lovás, M., Václavíková, M., Matik, M., Neubauer, M., 2004. Kinetics of grinding of secondary raw material serpentinite at cascade operating mode. Acta Montanistica Slovaca 9, 423–427.
Hredzák, S., Jakabský, Š., Lovás, M., Václavíková, M., Matik, M., Neubauer, M., 2005. Iron removal from secondary serpentinite raw material by high gradient magnetite separation. Chemical Papers 99, 84–87.
Huijgen, W.J.J., Witkamp, G.-J., Comans, R.N.J., 2005. Mineral CO_2 sequestration by steel slag carbonation. Environmental Science and Technology 39, 9676–9682.
Huijgen, W.J.J., Witkamp, G.J., Comans, R.N.J., 2006. Mechanisms of aqueous wollastonite carbonation as a possible CO_2 sequestration process. Chemical Engineering Science 61, 4242–4251.
Juhász, A.Z., Opoczky, L., 1990. Mechanical Activation of Minerals by Grinding: Pulverizing and Morphology of Particles. Ellis Horwood, Chichester, p. 234.
Kalinkina, E.V., Kalinkin, A.M., Forsling, W., Makarov, V.N., 2001. Sorption of atmospheric carbon dioxide and structural changes of Ca and Mg silicate minerals during grinding I. Diopside. International Journal of Mineral Processing 61, 273–288.
Kalinkin, A.M., Boldyrev, V.V., Politov, A.A., Kalinkina, E.V., Makarov, V.N., Kalinnikov, V.T., 2003. Investigation into the mechanism of interaction of calcium and magnesium silicates with carbon dioxide in the course of mechanical activation. Glass Physics and Chemistry 29, 410–414.
Kalinkin, A.M., Kalinkina, E.V., Politov, A.A., Makarov, V.N., Boldyrev, V.V., 2004. Mechanochemical interaction of Ca silicate and aluminosilicate minerals with carbon dioxide. Journal of Materials Science 39, 5393–5398.
Kleiv, R.A., Thornhill, M., 2006. Mechanical activation of olivine. Minerals Engineering 19, 340–347.

Kleiv, R.A., Sandvik, K.L., Thornhill, M., 2006. Increasing silicate carbonation kinetics by use of mechanical activation. In: Önal, G., et al. (Ed.), Proceeding of the XXIIIth International Mineral Procesing Congres. Istanbul, pp. 56–61.

Lackner, K.S., Wendt, C.H., Butt, D.P., Joyce, E.L., Sharp, D.H., 1995. Carbon dioxide disposal in carbonate minerals. Energy 20, 1153–1170.

Maroto-Valer, M.M., Fauth, D.J., Kuchta, M.E., Zhang, Y., Andrésen, J.M., 2005. Activation of magnesium rich minerals as carbonation feedstock materials for CO_2 sequestration. Fuel Processing Technology 86, 1627–1645.

Nakamoto, K., 1978. Infrared and Raman Spectra of Inorganic and Coordination Compounds. John Wiley and Sons, New York.

O'Connor, W.K., Dahlin, D.C., Turner, P.C., Walters, R.P., 1999. Carbon dioxide sequestration by ex-situ mineral carbonation. Technology 75, 115–123.

O'Connor, W.K., Dahlin, D.C., Nilsen, D.N., Rush, G.E., Walters, R.P., Turner, P.C., 2000. Carbon dioxide sequestration by direct mineral carbonation: Results from recent studies. Proc. Ist National Conference on Carbon Sequestration. Washington DC, NETL, 14 pp.

O'Connor, W.K., Dahlin, D.C., Rush, G.E., Dahlin, C.L., Collins, W.K., 2002. Carbon dioxide sequestration by direct mineral carbonation: process mineralogy of feed and products. Minerals and Metallurgical Processing 19, 95–101.

O'Connor, W.K., Dahlin, D.C., Rush, G.E., Gerdemann, S.J., Penner, L.R., 2004. Energy and economics considerations for ex-situ aqueous mineral carbonation. Proc. XXIXth International Technical Conference on Coal Ulitization and Fuel Systems, Coal Technology Association, Clearwater, Florida, 12 pp.

Ohlherg, S.M., Strickler, D.W., 1962. Determination of percent crystallinity of partly devitrified glass by X-ray diffraction. Journal of American Ceramic Society 45, 170–171.

Park, A.-H.A., Fan, L.-S., 2004. CO_2 mineral sequestration: physically activated dissolution of serpentine and pH swing process. Chemical Engineering Science 59, 5241–5247.

Pourghahramani, P., Forssberg, E., 2006a. Microstructure characterization of mechanically activated hematite using XRD line broadening. International Journal of Mineral Processing 79, 106–119.

Pourghahramani, P., Forssberg, E., 2006b. Comparative study of microstructural characteristics and stored energy of mechanically activated hematite in different grinding environments. International Journal of Mineral Processing 79, 120–139.

Seifritz, W., 1990. CO_2 disposal by means of silicates. Nature 345, 486.

Shi, J., Klocke, A., Zhang, M., Bismayer, U., 2005. Thermally-induced structural modification of dental enamel apatite: decomposition and transformation of carbonate groups. European Journal of Mineralogy 17, 769–775.

Summers, C.A., Dahlin, D.C., Rush, G.E., O'Connor, W.K., Gerdemann, S.J., 2005. Grinding methods to enhance the reactivity of olivine. Minerals & Metallurgical Processing 22, 140–144.

Tkáčová, K., 1989. Mechanical Activation of Minerals. Elsevier, Amsterdam.

Zhang, Q., Sugiyama, K., Saito, F., 1997. Enhancement of acid extraction of magnesium and silicon from serpentine by mechanochemical treatment. Hydrometallurgy 45, 323–331.